
The New Unidentified TeV Source in Cygnus (TeV J2032+4130): HEGRA IACT-System Results

Gavin Rowell¹, Dieter Horns¹, for the HEGRA Collaboration²

(1) *MPI für Kernphysik, Postfach 103980, D-69029 Heidelberg, Germany*

(2) *see <http://www-hegra.desy.de/hegra/>*

Abstract

The first unidentified TeV source in Cygnus is confirmed by follow-up observations carried out in 2002 with the HEGRA stereoscopic system of Čerenkov Telescopes. Using all ~ 279 hrs of data, this new source **TeV J2032+4130**, is steady over the four years of data taking, is extended with radius $6.2'$, and has a hard spectrum with photon index -1.9 . Its location places it at the edge of the core of the extremely dense OB association, Cygnus OB2. Its integral flux above energies $E > 1$ TeV amounts to $\sim 3\%$ of the Crab nebula flux. No counterpart at radio, optical and X-ray energies is as-yet seen, leaving TeV J2032+4130 presently unidentified. Summarised here are observational parameters of this source and brief astrophysical interpretation.

1. Introduction & Data Analysis

Analysis of archival data (~ 121 h) of the HEGRA system of Imaging Atmospheric Čerenkov Telescopes (HEGRA IACT-System see for e.g. [13]) devoted to the Cygnus region revealed the presence of a new TeV source [1]. This serendipitous discovery is now confirmed in follow-up observations from 2002 (~ 158 h) by the same telescopes. Given the lack of a counterpart at other energies, TeV J2032+4130 may represent a new class of particle accelerator.

For these analyses, cosmic-ray (CR) background events are rejected via a cut on the *mean-scaled-width* parameter \bar{w} [2]. Event directions are reconstructed using the so-called ‘algorithm 3’ [6], and a cut is made on the angular separation θ between the reconstructed event and assumed source direction. So-called *tight cuts* are implemented: $\theta < 0.12^\circ$, $\bar{w} < 1.1$, and also demanding a minimum $n_{\text{tel}} \geq 3$ images for the θ and \bar{w} calculation. The background is estimated using the *template* model [1,14], and consistent results are also obtained using an alternative *displaced* background model which employs ring-segments within the FoV. For the centre of gravity (CoG) and source extension determination, an additional cut on the estimated error in reconstructed direction ($\epsilon \leq 0.12^\circ$) is applied, reducing systematic effects (e.g. [7]). The CoG and source extension are estimated by fitting a 2D Gaussian convolved with the instrument’s point spread function to a

Table 1. Numerical summary for TeV J2032+4130 (preliminary). (a) Centre of Gravity (CoG) and extension σ_{src} (std. dev. of a 2D Gaussian); (b) Event summary. The values s and b are event numbers for the γ -ray-like and background (from the Template and Displaced models, see text) respectively, and $s - \alpha b$ is the excess using a normalisation α . S denotes the excess significance using Eq. 17 of [9]; (c) Events after spectral cuts; (d) Fitted power law.

(a) CoG & Extension ($\epsilon \leq 0.12^\circ$)				
RA α_{2000} :	20 ^{hr} 31 ^m 57.0 ^s		$\pm 6.2'_{\text{stat}}$	$\pm 13.7'_{\text{sys}}$
Dec δ_{2000} :	41 [°] 29' 56.8''		$\pm 1.1'_{\text{stat}}$	$\pm 1.0'_{\text{sys}}$
σ_{src}	6.2'		$\pm 1.2'_{\text{stat}}$	$\pm 0.9'_{\text{sys}}$

(c) Spectral Cuts: Tight Cuts + core \leq 200m					
Backgr.	s	b	α	$s - \alpha b$	S
— Energy estimation method: See [8] —					
Displaced	974	5122	0.143	242	+7.9

(b) Tight cuts: $\theta < 0.12^\circ$, $\bar{w} < 1.1$, $n_{\text{tel}} \geq 3$					
Backgr.	s	b	α	$s - \alpha b$	S
Template	1245	5926	0.168	252	+7.1
Displaced	1245	15492	0.065	243	+7.1

(d) Fitted Spectrum: Pure Power-Law	
dN/dE	$= N (E/1 \text{ TeV})^{-\gamma} \text{ ph cm}^{-2} \text{ s}^{-1} \text{ TeV}^{-1}$
N	$= 5.3 (\pm 2.2_{\text{stat}} \pm 1.3_{\text{sys}}) \times 10^{-13}$
γ	$= 1.9 (\pm 0.3_{\text{stat}} \pm 0.3_{\text{sys}})$

histogram of γ -ray-like ($\bar{w} < 1.1$) events binned over a $1^\circ \times 1^\circ$ FoV. At the CoG, the excess significance now exceeds 7σ from all 278.2 h of data, and the source extension is confirmed as non point-like. The reconstruction of event energy follows the method of [8] and we use tight cuts plus a cut on the reconstructed air-shower core distance of the event $core < 200$ m. A pure power law explains well the energy spectrum, showing no indication for a cut-off. A lower limit to the cut-off energy $E_c \sim 3.6, 4.2$ and 4.6 TeV is however estimated when fitting a power law+exponential cutoff term $\exp(-E/E_c)$ and fixing the power index at values $\gamma = 1.7, 1.9$ and 2.2 respectively. The integral flux for energies $E > 1$ TeV is $5.9 (\pm 3.1_{\text{stat}} \times 10^{-13})$, $\text{ph cm}^{-2} \text{ s}^{-1}$ or about 3% of the Crab nebula flux. Results are summarised in Table 1. and Fig 1. (upper panel).

2. Modelling TeV J2032+4130

Possible origins of TeV J2032+4130 have been discussed in literature [1,4, 12]. One interpretation involves association with the stellar winds of member stars in Cygnus OB2, individually or collectively, which provide conditions conducive to strong and stable shock formation for particle acceleration. Certainly the existence of TeV emission suggests particles accelerated to multi-TeV energies. We have therefore matched the spectral energy distribution of TeV J2032+4130 with coarse leptonic and hadronic models (Fig. 1. lower panel). Another scenario involves particle acceleration at a termination shock, which are expected at the boundary where a relativistic jet meets the interstellar medium. TeV J2032+4130 actually aligns well within the northern error cone of the bi-lobal jet of the famous microquasar Cygnus X-3 [10,11].

For simplicity we assume the TeV emission arises from either a pure sam-

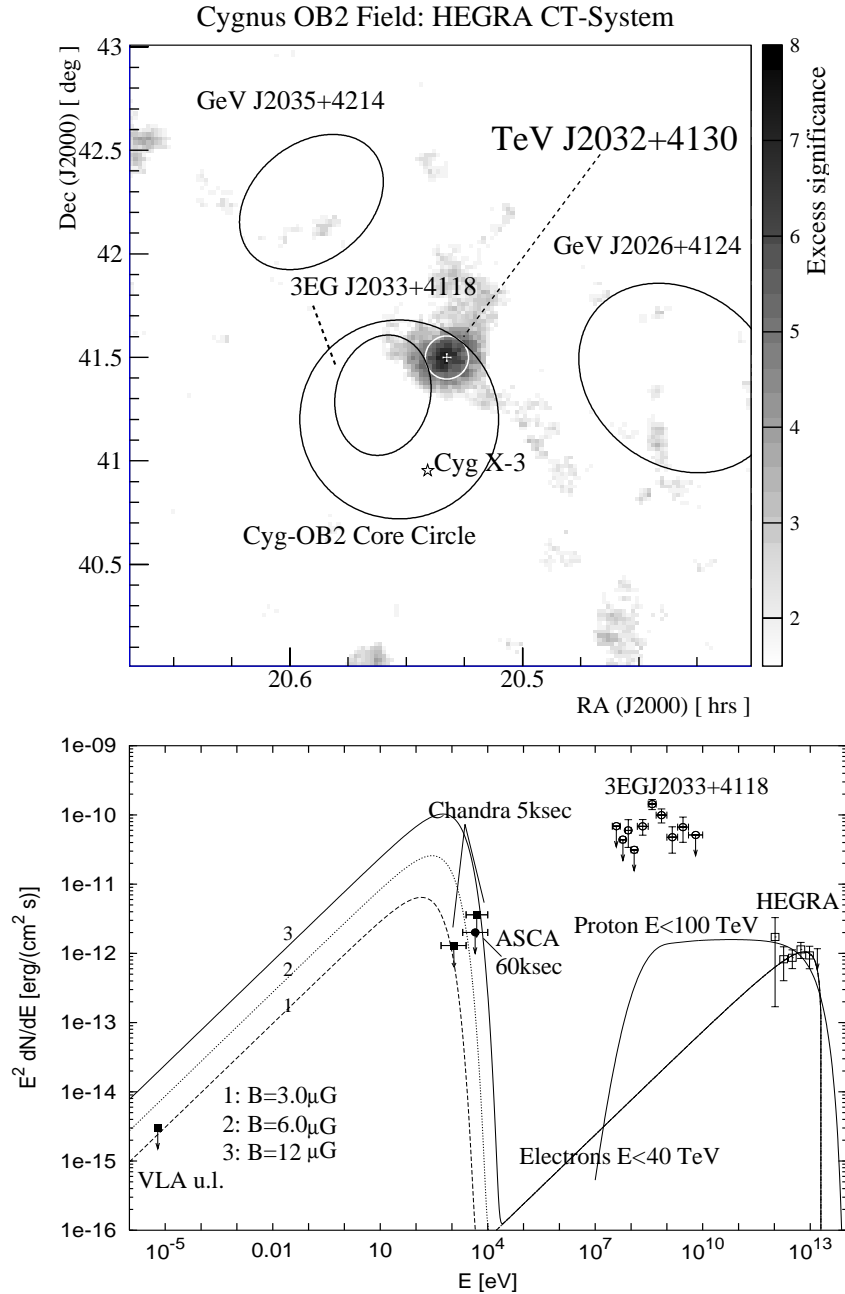


Fig. 1. **Upper:** Skymap of event excess significance (σ) from all HEGRA CT-System data ($3.0^\circ \times 3.0^\circ$ FoV) centred on TeV J2032+4130. Some nearby objects are indicated (GeV sources with 95% contours). The TeV source centre of gravity (CoG) with statistical errors, and error circle (65% confidence) for the extension (std. dev. of a 2D Gaussian, σ_{src}) are indicated by the white cross and white circle respectively. **Lower:** Spectrum of TeV J2032+4130 (labelled HEGRA) compared with purely hadronic (Protons $E < 100$ TeV) and leptonic (Electrons $E < 40$ TeV) models. Upper limits, constraining the synchrotron emission, are from the VLA and Chandra [3] and ASCA [1]. EGRET data points are from the 3rd EGRET catalogue [4].

ple of non-thermal hadronic or leptonic parent particles. Under the hadronic scenario the π^0 -decay prediction explains well the TeV flux when using a parent proton power law spectrum of index -2.0 with a sharp limit up to energies 100 TeV. The neighbouring EGRET source 3EG J2033+4118 (likely not related to TeV J2032+4130) provides no constraint on this model. Associated synchrotron X-ray emission would also be expected from tertiary electrons ($\pi^\pm \dots \rightarrow \mu^\pm \dots \rightarrow e^\pm \dots$). We have not yet modelled this component which essentially represents an absolute lower limit on any synchrotron emission visible. Assuming a pure leptonic scenario, TeV data are matched well by an inverse-Compton spectrum (up-scattering the cosmic microwave background) arising from an uncooled electron spectrum with power law index ~ -2.0 and hard cutoff at 40 TeV. This allows us to predict the synchrotron emission as a function of local magnetic field, constrained by the available upper limits at radio and X-ray energies. The most conservative synchrotron prediction arises from the $B_0 = 3.0\mu\text{G}$ choice, which is realistically the lowest such field expected in the Galactic disk. But in fact, much higher fields ($B_0 > 10\mu\text{G}$) are generally expected in such regions containing young/massive stars with high mass losses and colliding winds (e.g. [5]). Deep observations by XMM and Chandra will provide strong constraints on the leptonic component.

References

1. Aharonian F.A, et al. 2002 A&A 393, L37
2. Aharonian F.A, et al. 2000 ApJ 539, 317
3. Butt Y. et al. 2003 ApJ *submitted* (astro-ph/0302342)
4. EGRET Catalogue (3rd) <http://heasarc.gsfc.nasa.gov/>
5. Eichler D., Usov V. 1993 ApJ 402, 271
6. Hofmann W., et.al 1999 Astropart. Phys. 10, 275
7. Hofmann W., et.al 2000 A&A 361, 1073
8. Hofmann W., et.al 2000 Astropart. Phys. 12, 207
9. Li T.P., Ma Y.Q. 1983 ApJ 272, 317
10. Martí et al. 2000 ApJ 545, 939
11. Martí et al. 2001 A&A 375, 476
12. Mukherjee R. et al. 2003 ApJ *in press*, (astro-ph/0302130)
13. Pühlhofer G. et. al 2003 Astropart. Phys. *submitted*
14. Rowell G.P. 2003 A&A(Supp) *submitted*